ACS APPLIED MATERIALS & INTERFACES

Research Article

www.acsami.org

Self-Assembling Peptide of D-Amino Acids Boosts Selectivity and Antitumor Efficacy of 10-Hydroxycamptothecin

Jianfeng Liu,[‡] Jinjian Liu,[‡] Liping Chu,[‡] Yumin Zhang,[‡] Hongyan Xu,[‡] Deling Kong,[§] Zhimou Yang,[§] Cuihong Yang,[‡,*] and Dan Ding*[,§]

[‡]Tianjin Key Laboratory of Radiation Medicine and Molecular Nuclear Medicine, Institute of Radiation Medicine, Chinese Academy of Medical Science & Peking Union Medical College, Tianjin 300192, P. R. China

[§]State Key Laboratory of Medicinal Chemical Biology, Key Laboratory of Bioactive Materials, Ministry of Education, College of Life Sciences, and Collaborative Innovation Center of Chemical Science and Engineering (Tianjin), Nankai University, Tianjin 300071, P. R. China

Supporting Information

ABSTRACT: D-peptides, which consist of D-amino acids and can resist the hydrolysis catalyzed by endogenous peptidases, are one of the promising candidates for construction of peptide materials with enhanced biostability in vivo. In this paper, we report on a self-assembling supramolecular nanostructure of D-amino acid-based peptide Nap-G^{D}F^{D}F^{D}YGRGD (D-fiber, ^{D}F meant D-phenylalanine, ^{D}Y meant D-tyrosine), which were used as carriers for 10-hydroxycamptothecin (HCPT). Transmission electron microscopy observations demonstrated the filamentous morphology of the HCPT-loaded peptides (D-fiber-HCPT). The better selectivity and antitumor activity of D-fiber-HCPT than L-fiber-HCPT were found in the in vitro and in vivo antitumor studies. These results highlight that this model D-fiber system holds great promise as vehicles of hydrophobic drugs for cancer therapy.

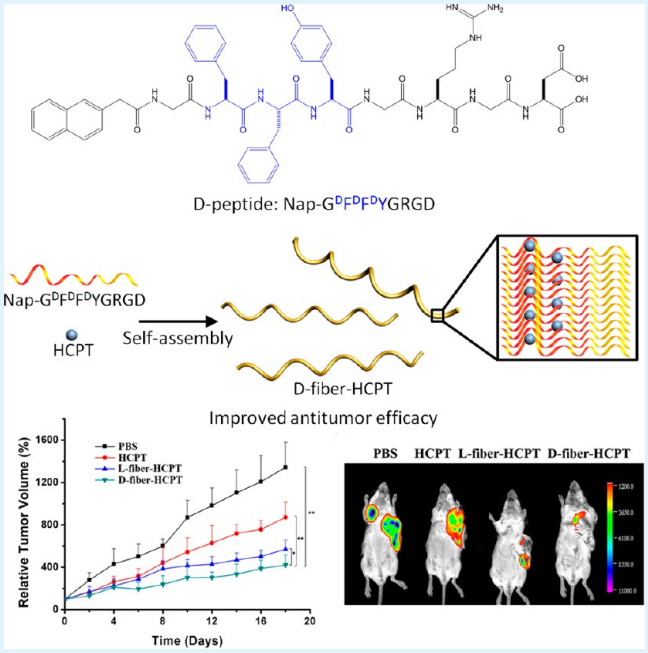

KEYWORDS: *D-peptide, self-assembly, nanofiber, hydrophobic drug delivery, 10-hydroxycamptothecin*

INTRODUCTION

Since the discovery of the first self-assembling peptide-EAK16 by Shuguang Zhang in 1989,[1] peptides that spontaneously undergo self-assembly into well-ordered nanofibers opened a new avenue for molecular fabrication of biomaterials.[2−6] Because of their good biocompatibility, easy modification by functional groups and design flexibility according to the needs through a "bottom-up" approach,[4] self-assembling peptide nanofibers have been widely used in cell culture,[7−10] disease diagnosis,[11,12] drug delivery,[13,14] tissue engineering,[15−17] and regenerative medicine research.[18,19] In the field of therapeutic drug delivery, self-assembling peptides have been explored as hydrophobic drug carriers with improved drug solubility, bioavailability and reduced toxicity.[20,21] For instance, Chen,[22,23] Pochan,[24] and Stupp[25] groups have developed self-assembling peptide nanostructures for delivery of hydrophobic antitumor agents, such as ellipticine, curcumin, and camptothecin. The application in controlled drug release requires that the peptide drug carriers are capable of resisting digestive enzymes and possessing long-term in vivo stability.[26,27] Despite the merits of self-assembling peptides in drug delivery, most of the peptide-based nanostructures made of natural amino acids are susceptible to degradation catalyzed by various endogenous proteases, which may lead to premature release of the loaded drugs and greatly limit their application in controlled drug delivery.[28−30] The introduction of D-amino acids, which can resist the proteases in vivo, is able to significantly increase the biostability of peptides.[29,31,32] Xu group has developed D-amino

Received: December 27, 2013
Accepted: March 24, 2014
Published: March 24, 2014

acid-based supramolecular hydrogels, which exhibited good controlled release characteristics after injection into the abdomens of rats[28] and D-peptide-based taxol-conjugated hydrogels showed higher anti-tumor efficacy as compared to the corresponding L-peptide control after local injection.[33,34] Encouraged by the recent progress and the very promising property of supramolecular nanostructures based on D-peptide derivatives, herein we designed cancer targeting ligand RGD-containing and L-/D-amino acid-based self-assembling peptides, Nap-GFFYGRGD and Nap-G^{D}F^{D}F^{D}YGRGD (L-fiber and D-fiber, respectively), as carriers for controlled delivery of 10-hydroxycamptothecin (HCPT). In this study, D-fiber has been demonstrated to be a more efficient HCPT vehicle for in vivo tumor growth inhibition as compared to L-fiber. This study thus opens up new opportunities for the development of a new generation of promising D-peptide-based nanomedicine for the advancement of cancer therapy.

MATERIALS AND METHODS

Materials. Rink amide-AM resin and Fmoc-amino acids were obtained from GL Biochem (Shanghai, China). Carbon-coated copper grids were purchased from Zhongjingkeyi Technology (Beijing, China). 3-(4,5-Dimethylthiazol-2-yl)-2,5-diphenyltetrazolium bromide (MTT), Roswell Park Memorial Institute 1640 Medium (RPMI-1640) and other reagents for cells culture were purchased from Gibco (GrandIsland, USA). 10-hydroxycamptothecin was purchased from Must Bio-Technology (Chengdu, China). In situ cell death detection kit (POD) was obtained from Roche (Basel, Switzerland). Other chemical reagents and solvents were obtained from Alfa (Shenzhen, China).

Cell Culture and Animal. NIH 3T3 (mouse embryonic fibroblast cells), EC 109 (esophageal squamous carcinoma cells) and 4T1-luciferase (luciferase-expressing mouse breast cancer cells) were cultured in RPMI-1640 medium supplemented with 10% fetal bovine serum (FBS), 100 U/mL penicillin, and 100 μg/mL streptomycin at 37 °C in 5% CO_2. Four- to five-week-old BALB/c mice (female) were purchased from Experimental Animal Center of Academy of Military Medical Sciences (Beijing, China). The animal studies were performed in accordance with the Regulations for the Administration of Affairs Concerning Experimental Animals (Tianjin, revised in June 2004) and adhered to the Guiding Principles in the Care and Use of Animals of the American Physiological Society.

Peptide Synthesis and Self-Assembling Properties Analysis. Peptides were prepared by standard solid phase peptide synthesis (SPPS) and purified by reverse phase high performance liquid chromatography (HPLC, LUMTECH, Germany) using a C_{18} RP column with MeOH (0.1% of TFA) and water (0.1% of TFA) as eluent. Nuclear magnetic resonance spectroscopy (^{1}H NMR, Bruker ARX 400, Switzerland) and high-resolution mass spectrometry (HR-MS, VG ZAB-HS system, England) were used to characterize the peptides. Peptide solutions were prepared by dissolving the peptide powder in phosphate buffered saline (PBS) buffer (pH 7.4), and then about 2.0 equiv. of Na_2CO_3 was added to neutralize the carboxylic acid groups on peptides. The self-assembly would take place during the cooling process to room temperature after being boiled. To study the self-assembling ability of the peptides, the critical micelle concentrations (CMC) of peptides in PBS buffer solutions were determined by dynamic light scattering (DLS) with a laser light scattering spectrometer (BI-200SM) equipped with a digital correlator (BI-9000AT) at 532 nm under room temperature (22-25 °C). Solutions containing different concentrations of peptides were tested, and the light scattering intensity was recorded for each concentrations analyzed.

Biostability Test of Nanofibers against Proteinase K. L- and D-fiber samples were prepared as described previously and the peptide concentration was 3 mg/mL. The nanofiber solution was diluted to 0.2 mg/mL for the biostability test against the proteinase K. Then proteinase K was added with the final concentration of 3.0 units/mL and incubated at 37 °C for 24 h. At predetermined time intervals, 400 μL of sample was taken out and then analyzed by HPLC and LC-MS.

Preparation of L-Fiber-HCPT and D-Fiber-HCPT. HCPT powers were dissolved in ethanol (5 mg/mL). Aliquots of HCPT-ethanol were transferred to a 1.5 mL centrifuge tube and dried in the super-clean worktable under flowing air. Peptide solution (3 mg/mL) was cooled to 60 °C after boiling and then added into the HCPT-contained tube and vortexed for 1 min, followed by keeping in a 60 °C water bath for 0.5 h in the dark. The resulting fiber-HCPT complex was kept at room temperature for 2 h. A centrifugation for 30 min at room temperature at 1500 g was then performed to sediment undissolved HCPT. The supernatant was then carefully collected and assayed for HCPT concentration using a standard curve method determined by the absorbance of HCPT at 266 nm in HPLC system.

Transmission Electron Microscope (TEM). Morphological characterization of the nanostructures was performed by TEM (Tecnai G20 F20, Amercia). The samples were prepared as follows: a 10 μL sample of L-fiber, D-fiber, L-fiber-HCPT, or D-fiber-HCPT was placed on a carbon-coated copper grid and incubated on the substrate for 30 s to allow the peptide nanostructures to adhere to the substrate, and rinsed with ultra-pure water twice; the moisture was then removed with absorbent paper. The sample plate was then stained with a saturated uranyl acetate solution and left in a desicator overnight before the measurement.

In Vitro HCPT Release. HCPT release studies were performed using dialysis method. One milliliters of L-fiber-HCPT or D-fiber-HCPT solution was added to a dialysis bag (molecular weight cut-off 1 kDa) and dialyzed against 20 mL of PBS buffer (pH 7.4) at 37 °C for 8 days. One milliliter of dialysate was taken out for quantitative research at each time point, and another 1 mL of fresh PBS buffer was added into the dialysate buffer. The amount of HCPT released from nanofibers was measured using fluorescence spectroscopy (Ex = 360 nm, Em = 450 nm).

Nile Blue Staining of Peptide Nanofiber and Cell Uptake Assay. Nile Blue power was dissolved in ultrapure water at concentration of 1 mg/mL. 5 μL of Nile Blue solution was added into 500 μL of peptide (3 mg/mL) during the cooling process of the peptide nanofiber formation. The stained D-fiber solution was diluted into 0.05 μg/mL by serum-free medium and then incubated with NIH 3T3 cells for 2 h. Fluorescence images of nanofiber and nanofiber-stained cells were subsequently taken by confocal microscopy.

In Vitro Cytotoxicity Assay. Cellular toxicities of the HCPT-loaded nanofibers were measured using the MTT assay. NIH 3T3, EC 109 and 4T1-luciferase cells were used in this study. Cells were seeded in 96-well plates at a density of 1×10^4 cells/well and cultured for 24 h. L-Fiber-HCPT and D-fiber-HCPT were prepared as above described with the peptide concentration of 3 mg/mL (HCPT feeding concentration of 0.5 mM). After removal of the non-loaded drug by centrifugation, the HCPT concentration in the nanofiber suspension was determined by HPLC. Subsequently, the samples of free HCPT, L-fiber-HCPT and D-fiber-HCPT were diluted by serum-free medium to a series of doses, respectively, on the basis of HCPT concentrations ranging from 0.016 to 16 μg/mL. Three types of cells were then exposed to the diluted samples at 37 °C, respectively. After incubation for 24 h, MTT assay were performed according to the supplier's instructions. The half maximal inhibitory concentration (IC_{50} value) was calculated according to the MTT results. In addition, the cytotoxicities of L- and D-fibers without encapsulation of HCPT (peptide concentration from 1 to 125 μg/mL) against three types of cell lines were also determined by the MTT assay.

In Vivo Evaluation of Antitumor Activity. The in vivo antitumor activity of L-fiber-HCPT and D-fiber-HCPT was evaluated on a mouse tumor model. Four- to five-week-old BALB/c mice (female) were inoculated with 4×10^5 4T1-luciferase cells subcutaneously on the flank to establish the xenograft tumors. Ten days after tumor implantation, the tumor volume reached about 200 mm^3 and the mice were randomly divided into four treatment groups (10 mice per group): PBS, free HCPT, L-fiber-HCPT, and D-fiber-HCPT. Free HCPT was dissolved in a 1% mixture consisting of polyethylene glycol 400, propylene glycol, and polysorbate 80

Scheme 1. (A) Chemical Structures of Nap-GFFYGRGD, Nap-G^{D}F^{D}F^{D}YGRGD, and 10-hydroxycamptothecin (HCPT); (B) Proposed Mechanism of L-/D-Nanofiber Formation and Their HCPT Encapsulation; (C) Schematic Illustration of Possible Mechanism That D-Nanofiber Possessed Better Biostability in Vivo As Compared to Its L-Counterpart

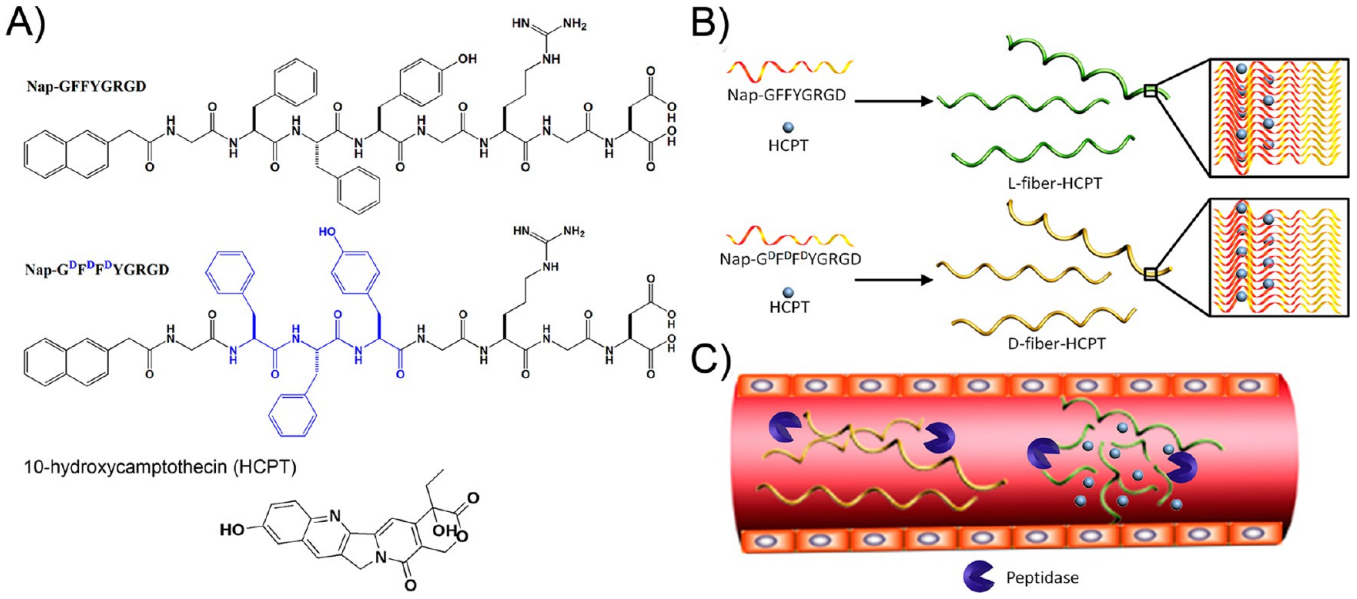

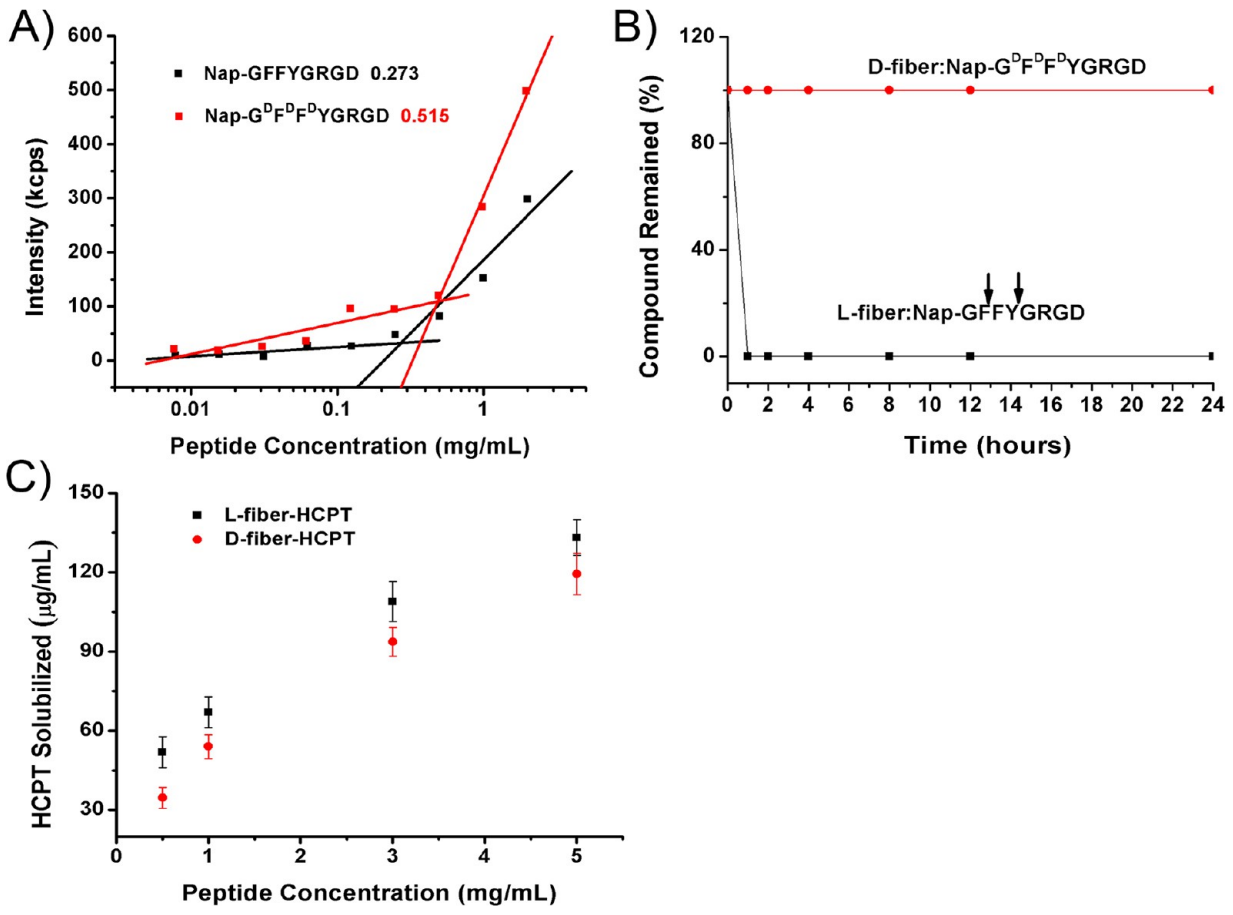

Figure 1. (A) Critical micelle concentration (CMC) of Nap-GFFYGRGD and Nap-G^{D}F^{D}F^{D}YGRGD, (B) stability of L-fiber and D-fiber against proteinase K digestion in PBS buffer solution (pH 7.4) (Compound concentration was 0.2 mg/mL; enzyme concentration was 3.0 units/mL; the arrows indicated the cleavage sites), and (C) HCPT concentration solubilized in L-fiber-HCPT and D-fiber-HCPT (The HCPT feeding concentration was 0.5 mM).

(40:58:2) in PBS v/v according to the literatures.[25] 2 mg/kg/dose of free HCPT or HCPT encapsulated in peptide nanofibers (3 mg/mL) was administrated via the tail vein every other day for six total administrations. Tumor growth was monitored every other day and

dx.doi.org/10.1021/am406007g | ACS Appl. Mater. Interfaces 2014, 6, 5558−5565

tumor volume was calculated by the formula: tumor volume (mm^3) = (length × $width^2$)×1/2. Twenty days after the first treatment, two 4T1-luciferase tumor bearing mice each group were received i.p. injection of 150 mg of D-luciferin/kg body weight (D-luciferin, firefly, potassium salt, SynChem, Inc.) and then anesthetized with 8% chloral hydrate. Ten minutes later, bioluminescent imaging of 4T1-luciferase tumor was performed using KODAK IS in vivo FX system according to the manufacturer's instructions. Additionally, the body weight and survival rate of mice in each group were also monitored for one month.

Histomorphological and Immunology Analysis. After the bioluminescent imaging experiment, mice were sacrificed and then tumor, liver, and spleen were collected. The samples were fixed for 24 h in 4% paraformaldehyde, embedded in paraffin, and cut into 8-μm-thick sections for haematoxylin & eosin (H&E) and in situ terminal deoxynucleotidyl transferase-mediated dUTP nick end labeling (TUNEL) assays according to the manufacturer's instructions. The photos were taken using optical microscope (Leica DMI6000 B). The numbers of apoptosis cells in tumor xnograft per field were counted (×200, $n = 6$), and the percent of apoptosis cells were calculated.

Statistical Analysis. All data are presented as mean ± standard deviation. An independent t-test was used for two-group comparisons, performed by SPSS 16.0 for Windows. $^*p < 0.05$ and $^{**}p < 0.001$ were used in this study to show statistical significance.

RESULTS AND DISCUSSION

Molecular Design. Many peptides based on the small dipeptide Phe-Phe (FF) are prone to self-assemble into nanostructures including nanofibers and nanospheres.[33,35] Our group has also demonstrated that Nap-GFFY is a good motif to construct self-assembling peptide-based gelators.[35] We therefore designed and synthesized Nap-GFFYGRGD and Nap-G^{D}F^{D}F^{D}YGRGD (Scheme 1A) as the possible self-assembling peptides for HCPT loading. The proposed mechanism of L-/D-nanofiber formation and their HCPT encapsulation was illustrated in Scheme 1B. The RGD motif in the peptide might have two functions. One is to increase the hydrophilicity of the resulting peptides for self-assembly purpose. The other is to endow the self-assembling nanofibers with active tumor-targeting ability. The two peptides could be easily obtained by standard Fmoc-solid phase peptide synthesis and purified by HPLC. The purity and identity of the peptides were characterized by ^{1}H NMR and HR-MS (see Figures S1–S4 in the Supporting Information).

Self-Assembling Ability, Biostability, and HCPT Encapsulation. After the successful synthesis of our designed compounds, we firstly tested their self-assembling abilities. Figure 1A showed that the CMC of Nap-GFFYGRGD and Nap-G^{D}F^{D}F^{D}YGRGD was 0.273 and 0.515 mg/mL, respectively, indicating that the replacement of FFY by the corresponding D-peptide ^{D}F^{D}F^{D}Y slightly weakened the self-assembly property of the designed peptide. The biostability of D- and L-peptide nanofibers was tested by the proteinase K disgestion method. As shown in Figure 1B, D-fiber possessed superb biostability against proteinase K. The intact chemical structure of D-peptide was maintained even after 24 h (see Figure S5 in the Supporting Information). In contrast, upon only 1 h incubation with proteinase K, almost all the L-peptides were cleaved by the enzyme with the cleavage sites between F and Y as well as G and F (see Figure S6 in the Supporting Information). These results indicated that D-nanofiber had better biostability against proteinase K as compared to its L-counterpart, which might be beneficial to its in vivo applications. Subsequently, the encapsulation of HCPT by the self-assembling nanofibers was qualitatively and quantitatively investigated. As shown in Figure S7 in the Supporting Information and Figure 1C, when the feeding concentration of HCPT was 0.5 mM and the peptide concentration was 3 mg/mL, loading efficiency of 73% and 66% was observed for L-peptide and D-peptide, respectively, which were comparable with that of the peptide amphiphile (PA) hydrophobic drug carrier system.[25] These results indicated that the HCPT encapsulation by the designed nanofibers of L-peptide and D-peptide could improve the aqueous solubility of HCPT more than 51- and 46-fold, respectively (with the solubility of 133 and 119 μg/mL as compared to that of free HCPT in water of 2.6 μg/mL). The quantitative results showed that the concentration of HCPT solubilized in the nanofibers of L-peptide or D-peptide increased with the increase of peptide concentration (Figure 1C). These results indicated that the feasibility of the designed peptide nanostructures as HCPT carriers.

Nanofiber Morphology. The morphology of the self-assembling peptide nanostructures was characterized by TEM. As shown in images A and B in Figure 2, both Nap-GFFYGRGD and Nap-G^{D}F^{D}F^{D}YGRGD peptides self-assembled into uniform nanofibers (L-fiber and D-fiber, respectively) with width of 10–20 nm and length of micrometer levels. Images C and D in Figure 2 showed the TEM images of HCPT-encapsulated L-fiber and D-fiber, respectively (L-fiber-HCPT and D-fiber-HCPT). Noteworthy is that similar morphologies were observed with and without HCPT encapsulation in the peptide fibers. These results suggested that the incorporation of HCPT into L-fiber and D-fiber has negligible interference on their self-assembling properties and morphologies. Furthermore, it would be noted that sedimentation of L-fiber-HCPT was observed at 2 weeks after HCPT encapsulation, but D-fiber-HCPT remained as a uniform solution for at least 4 weeks (Figure S8 in the Supporting Information). This result indicated that D-fiber-HCPT had the better storage stability as compared to L-fiber-HCPT.

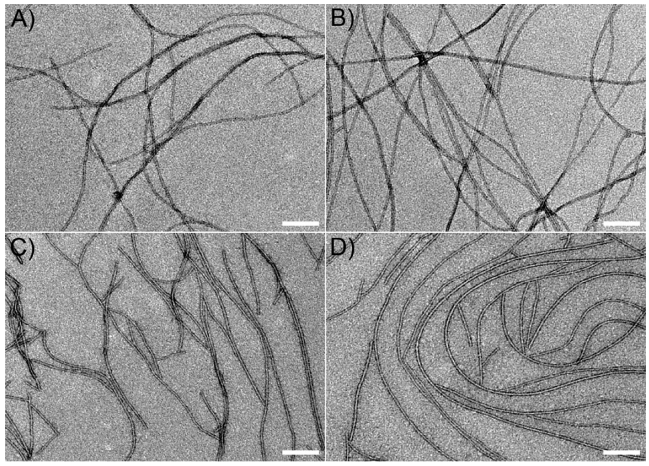

Figure 2. Transmission electron microscope (TEM) images of the nanostructures. (A) L-fiber, (B) D-fiber, (C) L-fiber-HCPT, and (D) D-fiber-HCPT. The scale bar was 100 nm for all the images.

In Vitro HCPT Release. The release profile of HCPT from the nanofibers was quantitatively studied over 1 week using dialysis method. As shown in Figure 3A, both L-fiber-HCPT and D-fiber-HCPT exhibited sustained and slow HCPT release

dx.doi.org/10.1021/am406007g | ACS Appl. Mater. Interfaces 2014, 6, 5558–5565

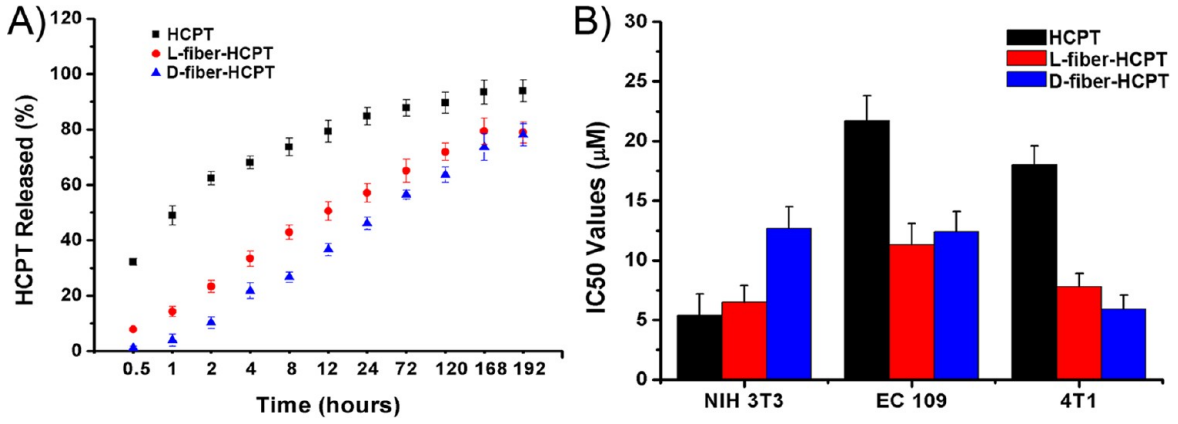

Figure 3. (A) In vitro HCPT release and (B) cytotoxicities of L-fiber-HCPT and D-fiber-HCPT.

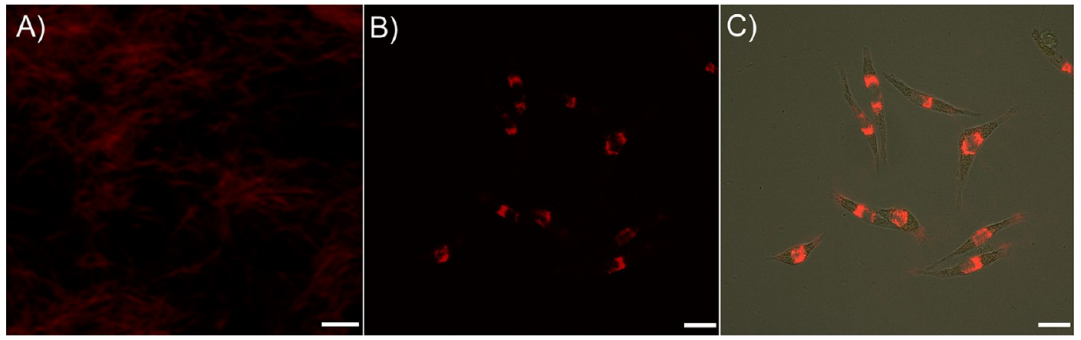

Figure 4. The Nile Blue staining of peptide nanofiber (A) and cell uptake of Nile Blue-stained nanofibers by NIH 3T3 cells (B, C). The scale bar is (A) 5 and (B, C) 25 μm.

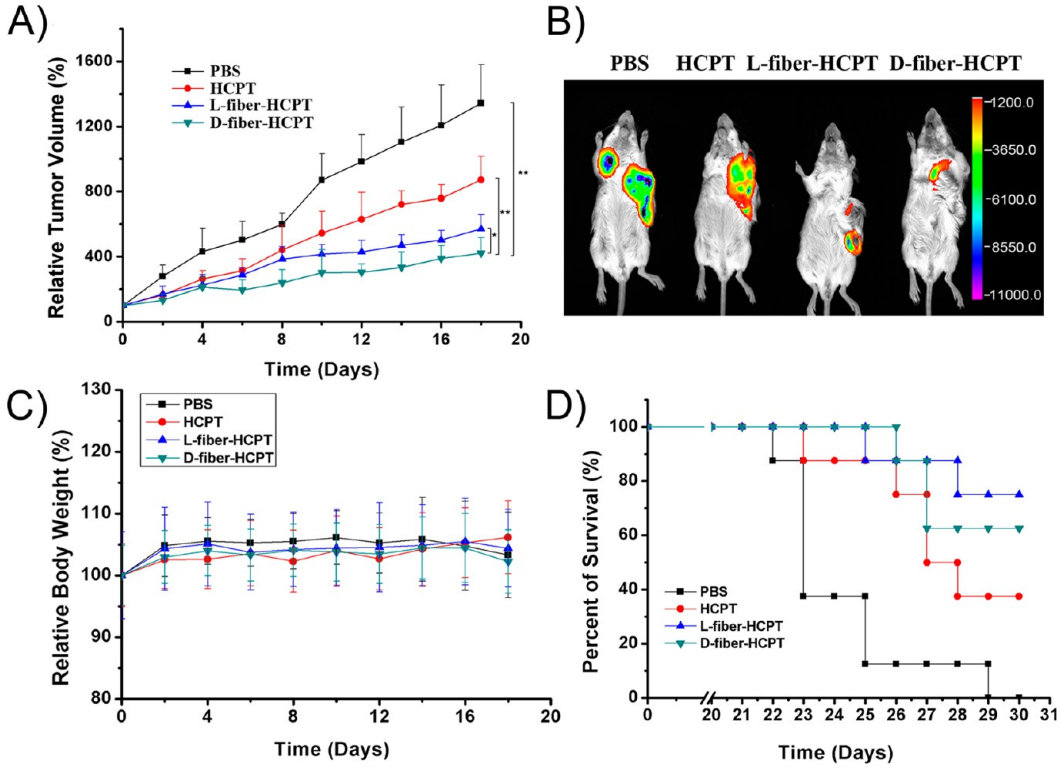

Figure 5. L-Fiber-HCPT and D-Fiber-HCPT inhibited 4T1-luciferase tumor xenograft growth in vivo. (A) Tumor inhibition curves, B) bioluminescent imaging on 4T1-luciferase tumor-bearing mice 20 days after given indicated treatments, (C) relative mouse weight over time during various treatments, and (D) Survival rate of mouse over time during various treatments. (*p = 0.018, ** p < 0.001, n = 8).

dx.doi.org/10.1021/am406007g | ACS Appl. Mater. Interfaces 2014, 6, 5558−5565

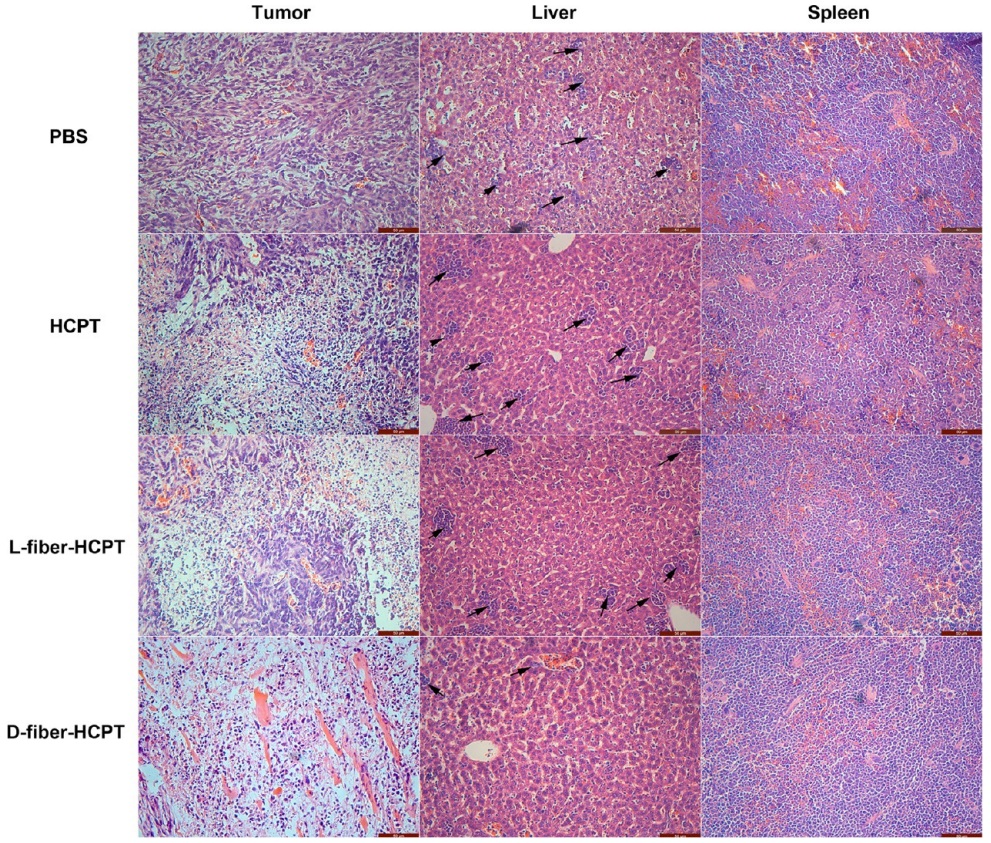

Figure 6. Haematoxylin & eosin (H&E) examination of tumor, liver, and spleen tissues from mice that received different treatments. The treatments were administrated via the tail vein every other day for six total times. Arrows indicate tumor metastases in liver, and the scale bar is 50 μm for all the images.

as compared to free HCPT. Briefly, in the first hour, 14.2 ± 1.8% and 3.9 ± 2.2% of HCPT was released from the L-fiber-HCPT and D-fiber-HCPT group, respectively. In comparison, 48.9 ± 3.5% of HCPT had been released from the free drug group. Moreover, Figure 3A also showed that D-fiber-HCPT had the better controlled drug release ability, which was consistent with the optical observations shown in Figure S8 in the Supporting Information. These results suggested that L-fiber-HCPT and D-fiber-HCPT could exhibit controlled drug release profile in vitro and unnatural D-peptides could increase the biostability and controlled release characteristics of the nanofibers.

Cytotoxicity and Cellular Uptake Study. To test the in vitro antitumor activity of the encapsulated HCPT, MTT assays toward the NIH 3T3, EC 109, and 4T1-luciferase cells were performed. Figure 3B showed that as compared to free HCPT, L-fiber-HCPT and D-fiber-HCPT had higher IC_{50} values for the normal cell line NIH 3T3, which possessed lower IC_{50} values for the cancer cell lines EC 109 and 4T1-luciferase. There was no significant difference in IC_{50} between L-fiber-HCPT and D-fiber-HCPT for cancer cell lines of EC 109 and 4T1-luciferase. Moreover, the empty L- and D-fibers without HCPT encapsulation showed low cytotoxicities against the three types of cell lines, indicating their good biocompatibility (see Figure S9 in the Supporting Information). These results suggested that the encapsulation of HCPT into the peptide nanofibers boosted the cancer cell selectivity of the drugs.

To investigate whether HCPT-loaded nanofibers can be internalized into the cells, the nanofibers were stained with Nile Blue, which had been widely applied to stain self-assembled nanostructures. As shown in Figure 4A, fluorescent nanofibers are clearly observed, indicating that the nanofibers could be well stained with Nile Blue. After incubation with Nile Blue-stained nanofibers for 2 h, NIH 3T3 cells were imaged by confocal microscopy. As shown in images B and C in Figure 4, it is obvious that fluorescence signal could be observed in the cytoplasm of NIH 3T3 cells, revealing the internalization of Nile Blue-stained nanofibers by the cells.

In Vivo Antitumor Activity Evaluation. The in vivo antitumor activities of L-fiber-HCPT and D-fiber-HCPT were investigated using a 4T1-luciferase xenograft model of breast cancer in BALB/c mice. Noteworthy is that no significant body weight changes were observed (Figure 5C) during various treatments, suggesting that the treatments did not diminish their overall health. Figure 5A showed significant reduction in tumor growth in the three treatment groups relative to the PBS control group. At day 18 post the first treatment, statistically significant difference ($p<0.001$) of the tumor growth inhibition effect was found in both L-fiber-HCPT and D-fiber-HCPT groups against free HCPT group. Figure 5A also showed that there was statistically difference ($p = 0.018$) between D-fiber-HCPT (relative tumor volume of 569.5 ± 87.4%) and L-fiber-HCPT (421.2 ± 94.9%). The superior therapeutic effect of L-fiber-HCPT and D-fiber-HCPT groups to that of free HCPT group could also be observed by bioluminescent imaging (Figure 5B) and by survival rate studies (Figure 5D). These results clearly indicated that the tumor inhibitory effect of HCPT was significantly improved by tumor-targeting peptide nanofibers as carriers. The better therapeutic effect of the nanofibers was probably due to the enhanced uptake of

dx.doi.org/10.1021/am406007g | ACS Appl. Mater. Interfaces 2014, 6, 5558−5565

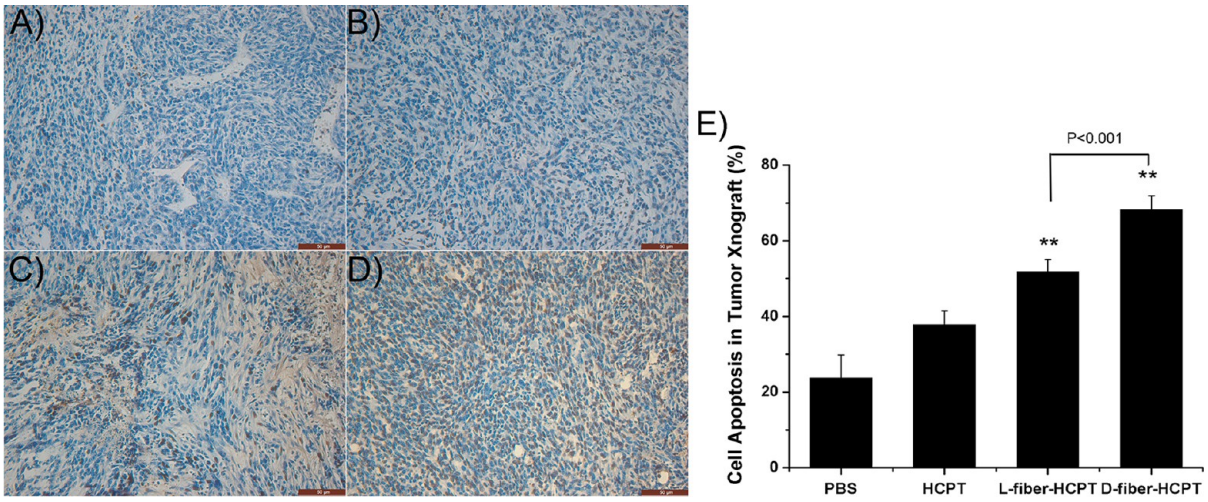

Figure 7. In situ terminal deoxynucleotidyl transferase-mediated dUTP nick end labeling (TUNEL) examination of tumor tissues from mice that received different treatments. (A) PBS, (B) free HCPT, (C) L-fiber-HCPT, (D) D-fiber-HCPT. (E) Quantitative analysis of TUNEL staining-positive cells in tumor xenografts from mice in various groups. The treatments were administrated via the tail vein every other day for six total times, ** $p < 0.001$ versus HCPT. The scale bar is 50 μm for all the images.

nanofibers by tumor tissue through the enhanced permeability and retention (EPR) effect[36] and the tumor-targeted delivery. Furthermore, the higher antitumor activity of D-fiber-HCPT as compared to L-fiber-HCPT may be ascribed to the relatively better biostability of D-peptides, probably because of the resistance of D-amino acids to the peptidases (Figure 1B), which would lead to the long-term drug release in vivo. Similar results was reported by Xu's group who found that D-peptide-based hydrogels exhibited higher antitumor efficacy than the L-peptides controls.[33]

H&E and TUNEL Assays. H&E and TUNEL assays were also performed to evaluate the antitumor efficacy and the toxicology of the HCPT-loaded nanofibers. H&E results of the breast cancer xenograft in Figure 6 indicated that more apoptotic or necrosis cells (with broken nucleis) were obviously found in both fiber-HCPT groups as compared to PBS and free HCPT groups. No apparent histopathological abnormalities or lesions in liver and spleen tissues were found in both fiber-HCPT groups, indicating the security of the nanofibers in vivo. It is noted that tumor metastases were observed in liver tissue for all the groups (indicated as arrows in Figure 6), revealing the malignance of tumor in this study. Encouragingly, the fewest tumor metastases were found in the D-fiber-HCPT group, indicating the highest inhibition effect of tumor metastases by D-fiber-HCPT. Figure 7 shows the TUNEL assay results. The nucleus were stained with hematoxylin and appeared as blue dots, the brown dots were the 3′3′-diaminobenzidine (DAB) signals that indicate apoptotic cells. As shown in images A and B in Figure 7, there were only few and sporadic brown dots shown in PBS control and free HCPT groups. In comparison, much more brown dots and brown regions that indicated the large number of apoptotic cells were observed for L-fiber-HCPT and D-fiber-HCPT groups (Figure 7C, D). Quantitative analysis of apoptotic cells in Figure 7E showed that the percentage of TUNEL-positive cells in PBS, free HCPT, L-fiber-HCPT, and D-fiber-HCPT group was 23.8 ± 6.0%, 37.9 ± 3.5%, 51.9 ± 3.2%, and 68.3±3.6%, respectively, indicating the best inhibition of tumor growth by D-fiber-HCPT. This result was consistent with the better tumor inhibition effect of the nanofiber groups in Figure 5, validating that the tumor inhibition ability of HCPT was significantly promoted by peptide nanofiber encapsulation.

CONCLUSIONS

In summary, we have developed L-/D-peptide nanofibers for controlled delivery of hydrophobic drug HCPT. The drug encapsulation process was performed in aqueous solution without any aid of organic solvents, which might decrease the toxicity of the resulting drug delivery systems. The results indicated that both L-peptide and D-peptide nanofibres could improve the aqueous solubility of HCPT. Moreover, D-fiber-HCPT showed a better long-term stability in aqueous solution as compared to L-fiber-HCPT. D-fiber-HCPT also exhibited better cancer cell selectivity in vitro and antitumor efficacy in vivo as compared to its L-counterpart. Although the mechanism of D-peptides that can act as more efficient drug carriers remains elusive, D-peptides have emerged as a novel drug delivery system and received great research interest. This successful example of D-fiber-HCPT that possessed superior antitumor activity to L-fiber-HCPT will inspire more exciting research in this emerging field. Considering the good performance of D-fiber-HCPT, further tuning the encapsulated hydrophobic drugs will facilitate the development of specific D-peptide-based nanomedicine for cancer therapy.

ASSOCIATED CONTENT

Supporting Information

Characterization of the peptides, HPLC chromatogram of the HCPT-encapsulated peptide nanofibers, optical images of L-fiber-HCPT and D-fiber-HCPT as well as in vitro cytotoxicities of empty L-/D-fibers. This material is available free of charge via the Internet at http://pubs.acs.org.

AUTHOR INFORMATION

Corresponding Authors

*E-mail: yangcuihong1983@163.com.
*E-mail: dingd@nankai.edu.cn.

Notes

The authors declare no competing financial interest.

■ ACKNOWLEDGMENTS

This work was supported by the Natural Science Foundation of China (51303213, 81301311, 81171371 and 51203189), Tianjin Science Foundation (13JCZDJC28100), PUMC Youth Fund and the Fundamental Research Funds for the Central Universities (3332013045) and the Development Foundation of IRM-CAMS (SF1417).

■ REFERENCES

(1) Zhang, S.; Holmes, T.; Lockshin, C.; Rich, A. Spontaneous Assembly of a Self-Complementary Oligopeptide to Form a Stable Macroscopic Membrane. *Proc. Natl. Acad. Sci. U.S.A.* **1993**, *90*, 3334−3338.

(2) Ulijn, R. V.; Smith, A. M. Designing Peptide Based Nanomaterials. *Chem. Soc. Rev.* **2008**, *37*, 664−675.

(3) Hauser, C. A.; Zhang, S. Designer Self-assembling Peptide Nanofiber Biological Materials. *Chem. Soc. Rev.* **2010**, *39*, 2780−2790.

(4) Ulijn, R. V.; Woolfson, D. N. Peptide and Protein Based Materials in 2010: from Design and Structure to Function and Application. *Chem. Soc. Rev.* **2010**, *39*, 3349−3350.

(5) Cui, H.; Webber, M. J.; Stupp, S. I. Self-assembly of Peptide Amphiphiles: from Molecules to Nanostructures to Biomaterials. *Biopolymers* **2010**, *94*, 1−18.

(6) Webber, M. J.; Kessler, J. A.; Stupp, S. I. Emerging Peptide Nanomedicine to Regenerate Tissues and Organs. *J. Intern. Med.* **2010**, *267*, 71−88.

(7) Yang, C.; Li, D.; Liu, Z.; Hong, G.; Zhang, J.; Kong, D.; Yang, Z. Responsive Small Molecular Hydrogels Based on Adamantane-Peptides for Cell Culture. *J. Phys. Chem. B* **2012**, *116*, 633−638.

(8) Zhou, M.; Smith, A. M.; Das, A. K.; Hodson, N. W.; Collins, R. F.; Ulijn, R. V.; Gough, J. E. Self-Assembled Peptide-Based Hydrogels as Scaffolds for Anchorage-dependent Cells. *Biomaterials* **2009**, *30*, 2523−2530.

(9) McClendon, M. T.; Stupp, S. I. Tubular Hydrogels of Circumferentially Aligned Nanofibers to Encapsulate and Orient Vascular Cells. *Biomaterials* **2012**, *33*, 5713−5722.

(10) Taskin, M. B.; Sasso, L.; Dimaki, M.; Svendsen, W. E.; Castillo-León, J. Combined Cell Culture-Biosensing Platform Using Vertically Aligned Patterned Peptide Nanofibers for Cellular Studies. *ACS Appl. Mater. Interfaces* **2013**, *5*, 3323−3328.

(11) Chen, C. S.; Xu, X. D.; Wang, Y.; Yang, J.; Jia, H. Z.; Cheng, H.; Chu, C. C.; Zhuo, R. X.; Zhang, X. Z. A Peptide Nanofibrous Indicator for Eye-Detectable Cancer Cell Identification. *Small* **2013**, *9*, 920−926.

(12) de la Rica, R.; Pejoux, C.; Fernandez-Sanchez, C.; Baldi, A.; Matsui, H. Peptide-Nanotube Biochips for Label-free Detection of Multiple Pathogens. *Small* **2010**, *6*, 1092−1095.

(13) Wang, H.; Wei, J.; Yang, C.; Zhao, H.; Li, D.; Yin, Z.; Yang, Z. The Inhibition of Tumor Growth and Metastasis by Self-Assembled Nanofibers of Taxol. *Biomaterials* **2012**, *33*, 5848−5853.

(14) Zhang, P. C.; Cheetham, A. G.; Lin, Y. A.; Cui, H. G. Self-Assembled Tat Nanofibers as Effective Drug Carrier and Transporter. *ACS Nano* **2013**, *7*, 5965−5977.

(15) Galler, K. M.; Hartgerink, J. D.; Cavender, A. C.; Schmalz, G.; D'Souza, R. N. A Customized Self-Assembling Peptide Hydrogel for Dental Pulp Tissue Engineering. *Tissue Eng. Part A* **2012**, *18*, 176−184.

(16) Akiyama, N.; Yamamoto-Fukuda, T.; Takahashi, H.; Koji, T. In Situ Tissue Engineering with Synthetic Self-Assembling Peptide Nanofiber Scaffolds, PuraMatrix, for Mucosal Regeneration in the Rat Middle-Ear. *Int. J. Nanomed.* **2013**, *8*, 2629−2640.

(17) Cheng, T. Y.; Chen, M. H.; Chang, W. H.; Huang, M. Y.; Wang, T. W. Neural Stem Cells Encapsulated in a Functionalized Self-Assembling Peptide Hydrogel for Brain Tissue Engineering. *Biomaterials* **2013**, *34*, 2005−2016.

(18) Gelain, F.; Horii, A.; Zhang, S. Designer Self-Assembling Peptide Scaffolds for 3-D Tissue Cell Cultures and Regenerative Medicine. *Macromol. Biosci.* **2007**, *7*, 544−551.

(19) Matson, J. B.; Stupp, S. I. Self-Assembling Peptide Scaffolds for Regenerative Medicine. *Chem. Commun. (Cambridge, U. K.).* **2012**, *48*, 26−33.

(20) Hartgerink, J. D.; Beniash, E.; Stupp, S. I. Peptide-Amphiphile Nanofibers: A Versatile Scaffold for the Preparation of Self-Assembling Materials. *Proc. Natl. Acad. Sci. U.S.A.* **2002**, *99*, 5133−5138.

(21) Altunbas, A.; Pochan, D. J. Peptide-Based and Polypeptide-Based Hydrogels for Drug Delivery and Tissue Engineering. *Top. Curr. Chem.* **2012**, *310*, 135−167.

(22) Sadatmousavi, P.; Mamo, T.; Chen, P. Diethylene Glycol Functionalized Self-Assembling Peptide Nanofibers and their Hydrophobic Drug Delivery Potential. *Acta Biomater.* **2012**, *8*, 3241−3250.

(23) Lu, S.; Wang, H.; Sheng, Y.; Liu, M.; Chen, P. Molecular Binding of Self-Assembling Peptide EAK16-II with Anticancer Agent EPT and Its Implication in Cancer Cell Inhibition. *J. Controlled Release* **2012**, *160*, 33−40.

(24) Altunbas, A.; Lee, S. J.; Rajasekaran, S. A.; Schneider, J. P.; Pochan, D. J. Encapsulation of Curcumin in Self-Assembling Peptide Hydrogels as Injectable Drug Delivery Vehicles. *Biomaterials* **2011**, *32*, 5906−5914.

(25) Soukasene, S.; Toft, D. J.; Moyer, T. J.; Lu, H.; Lee, H. K.; Standley, S. M.; Cryns, V. L.; Stupp, S. I. Antitumor Activity of Peptide Amphiphile Nanofiber-Encapsulated Camptothecin. *ACS Nano* **2011**, *5*, 9113−9121.

(26) Nagai, Y.; Unsworth, L. D.; Koutsopoulos, S.; Zhang, S. Slow Release of Molecules in Self-Assembling Peptide Nanofiber Scaffold. *J. Controlled Release* **2006**, *115*, 18−25.

(27) Williams, R. J.; Hall, T. E.; Glattauer, V.; White, J.; Pasic, P. J.; Sorensen, A. B.; Waddington, L.; McLean, K. M.; Currie, P. D.; Hartley, P. G. The in Vivo Performance of an Enzyme-Assisted Self-Assembled Peptide/Protein Hydrogel. *Biomaterials* **2011**, *32*, 5304−5310.

(28) Liang, G.; Yang, Z.; Zhang, R.; Li, L.; Fan, Y.; Kuang, Y.; Gao, Y.; Wang, T.; Lu, W. W.; Xu, B. Supramolecular Hydrogel of a D-Amino Acid Dipeptide for Controlled Drug Release in Vivo. *Langmuir* **2009**, *25*, 8419−8422.

(29) Luo, Z.; Wang, S.; Zhang, S. Fabrication of Self-Assembling D-Form Peptide Nanofiber Scaffold d-EAK16 for Rapid Hemostasis. *Biomaterials* **2011**, *32*, 2013−2020.

(30) Parween, S.; Ali, A.; Chauhan, V. S. Non-Natural Amino Acids Containing Peptide-Capped Gold Nanoparticles for Drug Delivery Application. *ACS Appl. Mater. Interfaces* **2013**, *5*, 6484−6493.

(31) Luo, Z.; Yue, Y.; Zhang, Y.; Yuan, X.; Gong, J.; Wang, L.; He, B.; Liu, Z.; Sun, Y.; Liu, J.; Hu, M.; Zheng, J. Designer D-Form Self-Assembling Peptide Nanofiber Scaffolds for 3-Dimensional Cell Cultures. *Biomaterials* **2013**, *34*, 4902−4913.

(32) Li, X.; Du, X.; Li, J.; Gao, Y.; Pan, Y.; Shi, J.; Zhou, N.; Xu, B. Introducing D-Amino Acid or Simple Glycoside into Small Peptides to Enable Supramolecular Hydrogelators to Resist Proteolysis. *Langmuir* **2012**, *28*, 13512−13517.

(33) Li, J.; Gao, Y.; Kuang, Y.; Shi, J.; Du, X.; Zhou, J.; Wang, H.; Yang, Z.; Xu, B. Dephosphorylation of D-Peptide Derivatives to Form Biofunctional, Supramolecular Nanofibers/Hydrogels and their Potential Applications for Intracellular Imaging and Intratumoral Chemotherapy. *J. Am. Chem. Soc.* **2013**, *135*, 9907−9914.

(34) Li, J.; Kuang, Y.; Gao, Y.; Du, X.; Shi, J.; Xu, B. D-Amino Acids Boost the Selectivity and Confer Supramolecular Hydrogels of a Nonsteroidal Anti-Inflammatory Drug (NSAID). *J. Am. Chem. Soc.* **2013**, *135*, 542−545.

(35) Wang, H.; Ren, C.; Song, Z.; Wang, L.; Chen, X.; Yang, Z. Enzyme-Triggered Self-Assembly of a Small Molecule: A Supramolecular Hydrogel with Leaf-Like Structures and an Ultra-Low Minimum Gelation Concentration. *Nanotechnology* **2010**, *21*, 225606.

(36) Christian, D. A.; Cai, S.; Garbuzenko, O. B.; Harada, T.; Zajac, A. L.; Minko, T.; Discher, D. E. Flexible Filaments for in Vivo Imaging and Delivery: Persistent Circulation of Filomicelles Opens the Dosage Window for Sustained Tumor Shrinkage. *Mol. Biopharm.* **2009**, *6*, 1343−1352.